Applied Mathematics Letters 127 (2022) 107844

Contents lists available at ScienceDirect

Applied Mathematics Letters

www.elsevier.com/locate/aml

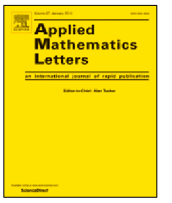

A spectral projection based method for the numerical solution of wave equations with memory

Christian Engström [a,*], Stefano Giani [b], Luka Grubišić [c]

[a] *Department of Mathematics, Linnaeus University, Växjö, 35195, Sweden*
[b] *Department of Engineering, Durham University, South Rd, Durham, DH13LE, United Kingdom*
[c] *Department of Mathematics, Faculty of Science, University of Zagreb, Bijenička 30, 10000 Zagreb, Croatia*

ARTICLE INFO

Article history:
Received 30 August 2021
Received in revised form 3 December 2021
Accepted 3 December 2021
Available online 9 December 2021

Keywords:
Inverse Laplace transform
Spectral projection
Wave equation with delay
Finite element approximation

ABSTRACT

In this paper, we compare two approaches to numerically approximate the solution of second-order Gurtin–Pipkin type of integro-differential equations. Both methods are based on a high-order Discontinous Galerkin approximation in space and the numerical inverse Laplace transform. In the first approach, we use functional calculus and the inverse Laplace transform to represent the solution. The spectral projections are then numerically computed and the approximation of the solution of the time-dependent problem is given by a summation of terms that are the product of projections of the data and the inverse Laplace transform of scalar functions. The second approach is the standard inverse Laplace transform technique. We show that the approach based on spectral projections can be very efficient when several time points are computed, and it is particularly interesting for parameter-dependent problems where the data or the kernel depends on a parameter.

1. Introduction

In this paper, we propose a numerical method for the wave equation

$$u_{tt} + Au - \int_0^t k(t-s)Au(s)ds = h, \tag{1.1}$$

which is based on a spectral decomposition of the positive self-adjoint operator A and the inverse Laplace transform. The operator A is by assumption elliptic and the spectrum of A consists of positive eigenvalues of finite multiplicities.

Wave equations with memory (1.1) are used to model heat transfer with finite propagation speed, systems with thermal memory, viscoelastic materials with a long memory, and acoustic waves in composite

* Corresponding author.
E-mail address: christian.engstrom@lnu.se (C. Engström).

https://doi.org/10.1016/j.aml.2021.107844

media [1,2]. Properties of the studied class of integro-differential equations were studied by many authors and we refer to [3] for a substantial presentation.

Several numerical methods for (1.1), and related equations, based on convolution quadrature [4,5] and the numerical inverse Laplace transform [6,7] have been developed over the last 25 years. The aim of the current study is to take advantage of the fact that A is a self-adjoint operator with discrete spectrum. Robust high-order finite element methods are well developed for approximating the eigenvalues and eigenvectors of A and we will in this work use the p-version of the symmetric interior penalty method [8]. The approximation of the solution of the time-dependent problem is then given by a summation of terms that are the product of the precomputed projections of the data and the inverse Laplace transform of scalar functions.

The Laplace transform of (1.1) results in an equation $T(\lambda)\hat{u} = \hat{f}$ and a numerical contour integral method is used to compute the inverse Laplace transform. The success and rate of convergence of the numerical inverse Laplace transform depend then crucially on the spectrum of the operator function T and the magnitude of the resolvent norm $\|T(\lambda)^{-1}\|$. In this paper, the infinite sum in the spectral decomposition of A is truncated, which results in a projected operator function T_N. The spectrum of T contains branches of eigenvalues with unbounded imaginary parts but the projected operator function T_N will only have spectral points with finite imaginary parts. This makes it straightforward to deform the contour in the Bromwich inversion formula into $\mathbb{C}^- := \{\lambda \in \mathbb{C} : \operatorname{Re}\lambda < 0\}$, which is Talbot's approach [9].

The projection-based approach described above is numerically compared with a standard inverse Laplace transform technique, which requires that many source problems be solved for each time point. A large part of the computations is in the projection-based approach independent of the data or point in time and we show that the approach can be very efficient when several time points are computed. The method is particularly interesting for parameter-dependent problems where the data are sufficiently smooth, or the kernel depends on a parameter. For the considered test case and implementation in MATLAB, the projection method is several orders of magnitude faster than the standard approach even if the precomputation time is included.

The paper is organized as follows. In Section 2 we present a representation formula for the solution, which includes eigenvalues and spectral projections of A, and an estimate of $\|T(\lambda)^{-1}\|$. In Section 3, we outline the standard approach inverse Laplace technique. Numerical results are presented in Section 4, and conclusions are stated in Section 5.

The presentation will for simplicity be restricted to $L^2(\Omega)$, where Ω denotes a bounded Lipschitz domain, and the case when A is a self-adjoint realization of the Laplace operator in $L^2(\Omega)$. We denote by $(\cdot,\cdot)$, $\|\cdot\|$ the inner product and norm in $L^2(\Omega)$, respectively.

The essential spectrum $\sigma_{\text{ess}}(B)$ of a closed operator B with domain $\operatorname{dom} B$ is defined as the set of all $\lambda \in \mathbb{C}$ such that $B - \lambda$ is not a Fredholm operator. Let T denote an operator function where $T(\lambda)$ for $\lambda \in \mathcal{D} \subset \mathbb{C}$ is an unbounded linear operator with domain $\operatorname{dom} T(\lambda)$. Then, the essential spectrum of T is the set

$$\sigma_{\text{ess}}(T) = \{\lambda \in \mathcal{D} : 0 \in \sigma_{\text{ess}}(T(\lambda))\}. \tag{1.2}$$

2. The spectral projection based method

The studied damped wave equation can then for $u = u(t) : [0,\infty] \to L^2(\Omega)$ formally be written in the form

$$u_{tt} - \Delta u + \int_0^t k(t-s)\Delta u(s)ds = h, \tag{2.1}$$

where $h : \mathbb{R}^+ \to L^2(\Omega)$, $k \in L_1(\mathbb{R}_+)$, and the initial data $u(x,0) = u_0(x)$, $u_t(x,0) = u_1(x)$ are in $L^2(\Omega)$. For simplicity, we restrict the study to Dirichlet conditions. Take $A : L^2(\Omega) \to L^2(\Omega)$ with domain $\operatorname{dom} A = \{u \in H_0^1(\Omega) : \Delta u \in L^2(\Omega)\}$ as the self-adjoint realization of the Laplace operator. Assume that $k \in L_1(\mathbb{R}_+)$ is non-negative, non-increasing, and $\int_0^\infty k(\tau)d\tau < 1$. Then (2.1) is well-posed in $L^2(\Omega)$.

Furthermore, for $h \equiv 0$, $u_0, u_1 \in \operatorname{dom} A$, we have $u \in C^1(\mathbb{R}_+; \operatorname{dom} A^{1/2})$; see [10] for further regularity results.

After applying the Laplace transform $\hat{f}(\lambda) = \int_0^\infty f(t)e^{-\lambda t}dt$ to (2.1) we formally obtain

$$T(\lambda)\hat{u} = \hat{h} + \lambda u_0 + u_1, \quad T(\lambda) = \lambda^2 + (1 - \hat{k}(\lambda))A.$$

The domain $\operatorname{dom} T$ of the closed operator function T must be $L^2(\Omega)$ for $\lambda \in \mathcal{D}$ with $\hat{g}(\lambda) = 0$, where $\hat{g}(\lambda) := 1 - \hat{k}(\lambda)$. Hence,

$$T(\lambda) = \lambda^2 + \hat{g}(\lambda)A, \quad \operatorname{dom} T(\lambda) = \begin{cases} L^2(\Omega) & \text{if } \hat{g}(\lambda) = 0, \\ \operatorname{dom} A & \text{otherwise.} \end{cases} \tag{2.2}$$

The following theorem is important for the numerical inverse Laplace transform computations.

Theorem 1. *The essential spectrum of the operator function T in (2.2) is $\sigma_{ess}(T) = \{\lambda \in \mathcal{D} : \hat{g}(\lambda) = 0\}$ and for $\lambda \notin \sigma(T)$, the following resolvent estimate holds*

$$\|T^{-1}(\lambda)\| \leq \frac{1}{|\hat{g}(\lambda)||\Im\hat{\gamma}(\lambda)|}, \quad \hat{\gamma}(\lambda) = -\frac{\lambda^2}{\hat{g}(\lambda)}.$$

Proof. The proof of characterization of the essential spectrum is a special case of Theorem 2.1 in [11]. Assume that $\lambda \notin \sigma(T)$. From the assumption that A is self-adjoint, it follows

$$|\hat{g}(\lambda)|\|T^{-1}(\lambda)\| = \|(A - \hat{\gamma}(\lambda))^{-1}\| = \frac{1}{\operatorname{dist}(\sigma(A), \hat{\gamma}(\lambda))}$$

and we can then estimate the norm as

$$\|T^{-1}(\lambda)\| \leq \frac{1}{|\hat{g}(\lambda)|\operatorname{dist}(\mathbb{R}, \hat{\gamma}(\lambda))} = \frac{1}{|\hat{g}(\lambda)||\Im\hat{\gamma}(\lambda)|}.$$

The advantage with the proposed resolvent estimate is that it is independent of the spectrum of the self-adjoint operator A and therefore can be approximated at low computational cost. From results in [3] and properties of the inverse Laplace transform, it can then be shown that the general solution of (2.1) can be represented as

$$u(t) = \frac{1}{2\pi i}\int_{r-i\infty}^{r+i\infty} e^{\lambda t}T(\lambda)^{-1}\hat{f}(\lambda)\,d\lambda, \quad \hat{f}(\lambda) = \hat{h} + \lambda u_0 + u_1. \tag{2.3}$$

The self-adjoint operator $(A, \operatorname{dom} A)$ has compact resolvent and spectrum $\sigma(A) = \{\mu_1, \mu_2, \dots\}$. Let P_j denote the spectral projection corresponding to the eigenvalue μ_j. Then, $T(\lambda)^{-1}$ can be represented as

$$T(\lambda)^{-1} = \sum_{j=1}^{\infty} K_j(\lambda, \mu_j)P_j, \quad K_j(\lambda, \mu_j) = \frac{1}{\lambda^2 + \mu_j(1 - \hat{k}(\lambda))}, \quad A = \sum_{j=1}^{\infty}\mu_j P_j. \tag{2.4}$$

Assume that $\hat{h}(x, \lambda) = \sum_{i=1}^{M}\hat{h}_i(\lambda)g_i(x)$. The solution of the time-dependent problem (2.1) can then be represented in the form

$$u(t) = \frac{1}{2\pi i}\sum_{j=1}^{\infty}\int_{r-i\infty}^{r+i\infty} e^{\lambda t}F_j(\lambda)\,d\lambda, \quad F_j(\lambda) = K_j(\lambda, \mu_j)\left[\sum_{i=1}^{M}\hat{h}_i(\lambda)P_j g_i + \lambda P_j u_0 + P_j u_1\right]. \tag{2.5}$$

Each term in the series (2.5) can then by linearity be written as a product of the operator P_j times the inverse Laplace transform of a scalar function $\hat{H}_j : \mathbb{C} \to \mathbb{C}$. In this paper, we base the numerical approximation

of (2.1) on the representation formula (2.5) (the projection approach) with T replaced by the projected operator function

$$T_N(\lambda) := \lambda^2 + (1 - \hat{k}(\lambda))A_N, \quad A_N = \sum_{j=1}^{N} \mu_j P_j. \tag{2.6}$$

Talbot's approach to numerically compute the inverse Laplace transform is to deform the standard contour in the Bromwich integral and several contours and quadrature formulas have been proposed; see [12,13]. In this paper we use

$$H_j(t) = \frac{1}{2\pi i} \int_{-\pi}^{\pi} \hat{H}_j(s(\alpha)) e^{s(\alpha)t} s'(\alpha)\, d\alpha, \quad s(\alpha) = \frac{2Q}{5t}\alpha(\cot\alpha + i), \quad -\pi < \alpha < \pi, \tag{2.7}$$

where Q is the number of quadrature points used in [14]. In the numerical simulations we use $k(t) = ae^{-bt}$ and compare with the standard approach that is based on (2.3). It can then be shown that $\sigma(T) \subset \mathbb{C}_-$, where the eigenvalues with non-zero imaginary part are enclosed in a vertical strip and $\sigma_{\text{ess}}(T) \subset \mathbb{R}_-$ [11]. Moreover, a derivation similar to [11, Lemma 2.6] shows then that the eigenvalues of T_N with non-zero imaginary part are enclosed by a finite vertical strip. Hence, it is always possible to choose $Q > 0$ such that s encloses all singularities in $T_N(\lambda)^{-1}$.

Let $\mathcal{V}_h^p$ denote the space of piece-wise polynomials of degree p on a triangulation $\mathcal{T}_h$ of Ω. The symmetric interior penalty method (SIP) is used to obtain the approximate eigenpairs $(\mu^h, v^h) \in \mathbb{R} \times \mathcal{V}_h^p$ of A. In the following, P_j^h denotes the discrete spectral projection associated to the single eigenvalue μ_j^h. For an eigenvalue μ_j of finite multiplicity, i.e dim $P_j(L^2(\Omega)) < \infty$, we have the following well known result

$$\delta(P_j^h(\mathcal{V}_h^p), P_j(L^2(\Omega))) \to 0, \quad \dim \mathcal{V}_h^p \to \infty,$$

where δ denotes the subspace gap [8]. This shows that we have no pollution of the eigenspaces and it is possible to show that the eigenvalues converge with double algebraic rate compared to the convergence of the eigenvectors. The original result from [8] was proved for h adaptive discontinuous Galerkin scheme, whereas the non-pollution result for the full hp-symmetric interior penalty discontinuous Galerkin finite element method has been obtained in [15, Section 3.1, Theorem 3.3.].

In the case of analytic eigenfunctions, there exist for the $p-$version of SIP constants $C_j > 0$ and $\gamma_j > 0$ such that

$$|\mu_j - \mu_j^h| \leq C_j e^{-2\gamma_j \sqrt{\dim \mathcal{V}_h^p}}.$$

For a detailed presentation of the method, we refer to [8,15,16].

Theorem 2. *Assume that $\hat{h}(x,\lambda) = \sum_{i=1}^{M} \hat{h}_i(\lambda) g_i(x)$ where h_i and K_j, as defined in (2.4), are regular and uniformly bounded along the path of integration in the inverse Laplace transform. Furthermore, assume that*

$$\|u_0 - \sum_{j=1}^{N} P_j^h u_0\| \leq \epsilon_0, \quad \|u_1 - \sum_{j=1}^{N} P_j^h u_1\| \leq \epsilon_1 \quad \|g_i - \sum_{j=1}^{N} P_j^h g_i\| \leq \epsilon_{g_i}, \tag{2.8}$$

where P_j^h denotes the approximate projection operator. Set $C_f = \max_j |\mathcal{L}^{-1}(K_j f)|$, where $\mathcal{L}^{-1}$ denotes the inverse Laplace transform and let u_N^h denote the approximate solution using the projected operator function (2.6). Then, for sufficiently large finite element space $\mathcal{V}_h^p$ and N, the following asymptotic error estimate holds to the first order

$$\|u - u_N^h\| \lesssim \sum_{i=1}^{M} \epsilon_{g_i} C_{\hat{h}_i} + \epsilon_0 C_\lambda + \epsilon_1 C_1. \tag{2.9}$$

Proof. The exact solution can be written in the form $u(x,t) = G_\infty + U_\infty + V_\infty$, where

$$G_N = \sum_{j=1}^{N} \mathcal{L}^{-1}(K_j(\lambda,\mu_j) \sum_{i=1}^{M} \hat{h}_i(\lambda) P_j g_i), \quad U_N = \sum_{j=1}^{N} \mathcal{L}^{-1}(\lambda K_j(\lambda,\mu_j)) P_j u_0,$$
$$V_N = \sum_{j=1}^{N} \mathcal{L}^{-1}(K_j(\lambda,\mu_j)) P_j u_1.$$

The corresponding approximate operators are denoted by

$$G_N^h = \sum_{j=1}^{N} \mathcal{L}^{-1}(K_j(\lambda,\mu_j^h) \sum_{i=1}^{M} \hat{h}_i(\lambda) P_j^h g_i), \quad U_N^h = \sum_{j=1}^{N} \mathcal{L}^{-1}(\lambda K_j(\lambda,\mu_j^h)) P_j^h u_0,$$
$$V_N^h = \sum_{j=1}^{N} \mathcal{L}^{-1}(K_j(\lambda,\mu_j^h)) P_j^h u_1.$$

Let $\mu_j = \mu_j^h + \epsilon_j$, where μ_j^h denotes an approximate eigenvalue of A, and assume that ϵ_j is sufficient small. Then a Taylor expansion gives

$$K_j(\lambda,\mu_j) = K_j(\lambda,\mu_j^h) + \epsilon_j K_j^1(\lambda,\mu_j^h) + \cdots, \quad K_j^1(\lambda,\mu_j^h) = -\frac{1-\hat{k}(\lambda)}{[\lambda^2 + \mu_j^h(1-\hat{k}(\lambda))]^2}.$$

The proposed estimate is based on the leading order terms in the expansion. We have

$$u - u_h = G_\infty - G_N^h + U_\infty - U_N^h + V_\infty - V_N^h,$$

where to the first order

$$G_\infty - G_N^h = \sum_{j=1}^{N} \mathcal{L}^{-1}(K_j(\lambda,\mu_j^h) \sum_{i=1}^{M} \hat{h}_i(\lambda)(P_j - P_j^h) g_i) + \sum_{j=1+N}^{\infty} \epsilon_j \mathcal{L}^{-1}(K_j^1(\lambda,\mu_j^h) \sum_{i=1}^{M} \hat{h}_i(\lambda) P_j g_i),$$
$$U_\infty - U_N^h = \sum_{j=1}^{N} \mathcal{L}^{-1}(K_j(\lambda,\mu_j^h)\lambda)(P_j - P_j^h) u_0 + \sum_{j=1+N}^{\infty} \epsilon_j \mathcal{L}^{-1}(K_j^1(\lambda,\mu_j^h)\lambda) P_j u_0,$$
$$V_\infty - V_N^h = \sum_{j=1}^{N} \mathcal{L}^{-1}(K_j(\lambda,\mu_j^h))(P_j - P_j^h) u_1 + \sum_{j=1+N}^{\infty} \epsilon_j \mathcal{L}^{-1}(K_j^1(\lambda,\mu_j^h)) P_j u_1.$$

Then

$$\|U_\infty - U_N^h\| = \|\sum_{j=1}^{N} \alpha_j (P_j - P_j^h) u_0 + \sum_{j=1+N}^{\infty} \beta_j P_j u_0\|, \quad \alpha_j = \mathcal{L}^{-1}(K_j(\lambda,\mu_j^h)\lambda),$$
$$\beta_j = \epsilon_j \mathcal{L}^{-1}(K_j^1(\lambda,\mu_j^h)\lambda),$$

where

$$\|\sum_{j=1}^{N} (P_j - P_j^h) u_0 + \sum_{j=N+1}^{\infty} P_j u_0\| \le \epsilon_0.$$

The term $|\beta_j|$ goes rapidly to zero as $N+1 \le j \to \infty$. Therefore, we may in the derivation of the asymptotic estimate assume that $|\beta_j| < \max|\alpha_j|$ and set $C_\lambda := \max|\alpha_j|$. Then, we obtain

$$\|U_\infty - U_N^h\| \le \epsilon_0 C_\lambda,$$

and the remaining terms in (2.9) are derived similarly.

3. The standard approach

The standard approach, based on a direct discretization of (2.3) or similar problems, has been studied by many authors, including [5,6,17,18]. It is not clear that Talbot's approach will work well for the studied wave equation, since the imaginary part of eigenvalues of T can be arbitrarily large. Hence, the discrete problem may have eigenvalues with very large imaginary part. As a consequence, a curve s that encloses all singularities in the matrix function $T^h(\lambda)^{-1}$ must be very long, which requires many quadrature points. However, the numerical results using the standard approach are mainly used for comparison of speed and we will therefore present numerical results based on a discretization of

$$u(t) = \frac{1}{2\pi i}\int_{-\pi}^{\pi} e^{s(\alpha)t}s'(\alpha)T^{-1}(s(\alpha))f(s(\alpha))\,d\alpha, \tag{3.1}$$

where the same contour s and the same number of quadrature points are used for both methods.

Our numerical simulations show that the method based $(T^h)^{-1}$ on also produces accurate results for the test case even if the contour does not enclose all singularities in $(T^h)^{-1}$. However, the estimate in Theorem 2 does only apply to the projection based method. A significant difference between the two approaches is that (3.1) requires the solution of a large number of source problems, whereas in the discretization of (2.5) it is only necessary to compute the inverse Laplace transform of scalar functions and sum up terms from precomputed series expansions of the given data.

4. Numerical results

In this section we compare our current implementations in MATLAB of the projection approach with the standard approach. The computational platform is a Laptop with 16 Gb RAM and an i7-7700HQ CPU @ 2.80 GHz. The precomputation steps in the projection approach consist of

1. Approximate the eigenpairs of A corresponding to the smallest eigenvalues using the symmetric interior penalty method
2. Determine an orthonormal basis of eigenvectors
3. Determine the eigenvalues with largest imaginary part of the reduced operator function T_N^h
4. Choose a curve that encloses the spectrum of the reduced operator function T_N^h
5. Compute an upper bound of the resolvent of the reduced operator function T_N^h over the curve

In the online phase, we

1. Project the data on the computed span of the eigenvectors
2. Compute the numerical inverse Laplace transform of the scalar functions in the representation formula (2.5)
3. Sum up the terms, where the terms consist of products of the terms in (2) and the projected data from (1)
4. Compute simultaneously to 3. the global error estimator in Theorem 2

It may in some applications also be possible to compute the inverse Laplace transforms before the online step. This would significantly speed up the online computations, but we will not consider that possibility in the comparison with the standard approach.

We choose $\Omega = (0,1)^2$ and the data such that the exact solution of (2.1) is given by

$$u(x,t) = h_1(t)g_1(x) + h_2(t)g_2(x), \tag{4.1}$$

where

$$h_1(t) = 1, \quad h_2(t) = -t^2e^{-t}, \quad g_1(x) = \sin(n_0\pi x_1)\sin(m_0\pi x_2), \quad g_2(x) = (x_1x_2)^a(1-x_1)^b(1-x_2)^b. \tag{4.2}$$

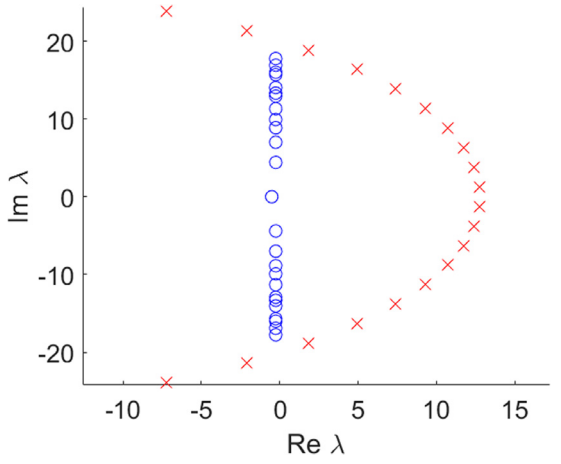

Fig. 1. Talbot curve when $t = 1$ and spectrum of reduced operator function (2.6) using $N = 20$. The computed eigenvalues are marked with ∘ and × are quadrature points on the contour s.

Set $k(t) = 0.5e^{-t}$. The operator function, which is defined for all $\lambda \in \mathbb{C} \setminus \{-1\}$, is then rational:

$$T(\lambda) = \lambda^2 + \left(1 - \frac{1}{2}\frac{1}{1+\lambda}\right) A, \quad \operatorname{dom} T(\lambda) = \begin{cases} L^2(\Omega) & \text{if } \lambda = -\frac{1}{2}, \\ \operatorname{dom} A & \text{otherwise.} \end{cases}$$

The spectrum $\sigma(T)$ consists of the essential spectrum $\sigma_{\text{ess}}(T) = \{-1/2\}$ and complex eigenvalues of finite multiplicity that have negative real part. It is possible to enclose the spectrum using results from [11], but we will for illustration purposes numerically compute the eigenvalues with non-zero imaginary part; see [19]. The projection method will be based on at most $N = 10$ projections, corresponding to the approximations of the lowest eigenvalues of $A := -\Delta$. Fig. 1 depicts quadrature nodes on the chosen Talbot curve when $Q = 32$ quadrature points are used and $t = 1$. A discretization of the estimate in Theorem 1 shows that norm of the resolvent T_N^{-1} (and its discretization) for points on the Talbot curve is

$$\max_{\alpha} \|T_N(s(\alpha))^{-1}\| \leq 0.51.$$

Hence, the resolvent is well behaved along the integration path.

Fig. 2 depicts the L_2-error and the estimated L_2-error from Theorem 2 for two different discretizations, when the reduced operator function is based on $N = 1, 2, \ldots, 10$ projections and the exact solution is (4.1). A coarse mesh with 36 triangles was used in all computations. Note that the exact solution in Case 2 oscillates less than in Case 1 but a lower polynomial degree is used ($p = 6$, DOFs= 1008 in Case 2 and $p = 10$, DOFs= 2376 in Case 1). As a result we obtain small errors in Case 2 using only the projection corresponding to the lowest eigenvalue but the error is smaller for Case 1 if $N \geq 6$. Moreover, the estimated L_2-error follows the exact error even if the exact error is of order one.

Table 1 presents the total computational time for 10 points in time using different finite element spaces. The times in parenthesis under the *Projection* approach include the precomputation of an ON-basis. For both approaches, we use $N = 10$ in the SIP approximation and 32 quadrature nodes in the numerical inverse Laplace transform. A coarse mesh with 36 triangles was used in the computations of the first two rows from the top with $p = 3$ in row one and $p = 10$ in row two. A finer mesh with 3766 triangles was used for the lowest two rows with $p = 2$ in row three and $p = 4$ in row four. The errors for the two approaches are very similar but the projection method is much faster. The column *Factor* indicates the speed up of the projection approach compared with the *Standard* approach with the current implementation in MATLAB. Those factors depend on the hardware, the implementation, and the problem.

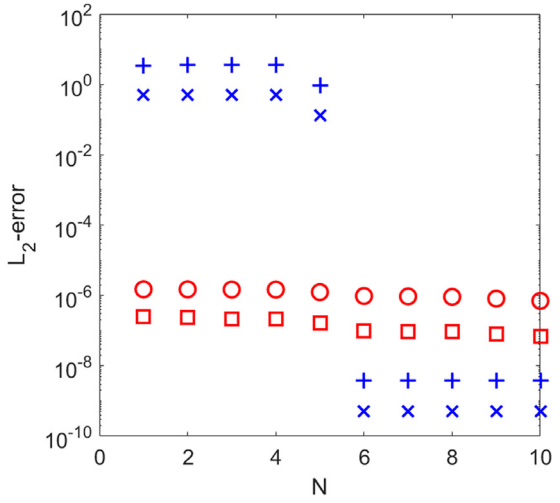

Fig. 2. The L_2-error and the error estimator in Theorem 2 for the problem (4.1), with $t = 1$, as a function of the number of projections N in the reduced operator function (2.6). Case 1: $p = 10$, $a = b = 8$, $n_0 = 3$, and $m_0 = 1$. The exact L_2-errors are marked with $\times$ and $+$ is the error estimator. Case 2: $p = 6$, $a = 4$, $b = 5$, $n_0 = m_0 = 1$. The exact L_2-errors are marked with $\square$ and $\circ$ is the error estimator.

Table 1
Total computational time in seconds for 10 points in time and different discretizations. The numbers in parenthesis include the precomputation of an ON-basis. The L_2-errors for the standard and the projection approach are very similar.

The Unit square			
dofs	Standard	Projection	Factor
360	0.83	0.19 (0.54)	4.4 (1.5)
2376	11	0.21 (0.76)	52 (14)
22596	51	0.61 (2.69)	83 (19)
56490	301	0.68 (5.28)	442 (57)

5. Conclusions

We have presented a numerical method for integro-differential equations based on a spectral decomposition and the inverse Laplace transform. This approach avoids the bottleneck in the standard approach, which is that we need to solve a large number of linear systems when we compute the numerical inverse Laplace transform. The proposed method projects the data on the span of a selection of eigenvectors and we showed numerically that the proposed global error estimate follows the exact error also for coarse discretizations. Alternative approaches include methods based on a Proper Orthogonal Decomposition (POD), which also could lead to a significant speedup, but at the cost of a much longer precomputation step.

Acknowledgments

CE was supported by the Swedish Research Council under Grant No. 2021-04537. LG was supported by the Hrvatska Zaklada za Znanost (Croatian Science Foundation) under the grant IP-2019-04-6268 - Randomized low-rank algorithms and applications to parameter dependent problems.

References

[1] M.E. Gurtin, A.C. Pipkin, A general theory of heat conduction with finite wave speeds, Arch. Ration. Mech. Anal. 31 (2) (1968) 113–126, http://dx.doi.org/10.1007/BF00281373, URL https://doi.org/10.1007/BF00281373.

[2] R. Dautray, J.-L. Lions, Mathematical Analysis and Numerical Methods for Science and Technology, Vol. 1, Springer-Verlag, Berlin, 1990, p. xviii+695, Physical origins and classical methods, With the collaboration of Philippe Bénilan, Michel Cessenat, André Gervat, Alain Kavenoky and Hélène Lanchon, Translated from the French by Ian N. Sneddon, With a preface by Jean Teillac.
[3] J. Prüss, Evolutionary Integral Equations and Applications, in: Monographs in Mathematics, Vol. 87, Birkhäuser Verlag, Basel, 1993, p. xxvi+366, http://dx.doi.org/10.1007/978-3-0348-8570-6, URL https://doi.org/10.1007/978-3-0348-8570-6.
[4] D. Xu, Decay properties for the numerical solutions of a partial differential equation with memory, J. Sci. Comput. 62 (1) (2015) 146–178, http://dx.doi.org/10.1007/s10915-014-9850-0, URL https://doi.org/10.1007/s10915-014-9850-0.
[5] K. Mustapha, D. Schötzau, Well-posedness of *hp*-version discontinuous Galerkin methods for fractional diffusion wave equations, IMA J. Numer. Anal. 34 (4) (2014) 1426–1446, http://dx.doi.org/10.1093/imanum/drt048, URL https://doi.org/10.1093/imanum/drt048.
[6] W. Mclean, V. Thomée, Numerical solution via Laplace transforms of a fractional order evolution equation, J. Integral Equations Appl. 22 (1) (2010) 57–94, http://dx.doi.org/10.1216/JIE-2010-22-1-57, URL https://doi.org/10.1216/JIE-2010-22-1-57.
[7] S.-L. Wu, Laplace inversion for the solution of an abstract heat equation without the forward transform of the source term, J. Numer. Math. 25 (3) (2017) 185–198, http://dx.doi.org/10.1515/jnma-2016-1014, URL https://doi.org/10.1515/jnma-2016-1014.
[8] P.F. Antonietti, A. Buffa, I. Perugia, Discontinuous Galerkin approximation of the Laplace eigenproblem, Comput. Methods Appl. Mech. Engrg. 195 (25–28) (2006) 3483–3503, http://dx.doi.org/10.1016/j.cma.2005.06.023, URL https://doi.org/10.1016/j.cma.2005.06.023.
[9] A. Talbot, The accurate numerical inversion of Laplace transforms, J. Inst. Math. Appl. 23 (1) (1979) 97–120.
[10] J. Prüss, Decay properties for the solutions of a partial differential equation with memory, Arch. Math. (Basel) 92 (2) (2009) 158–173, http://dx.doi.org/10.1007/s00013-008-2936-x, URL https://doi.org/10.1007/s00013-008-2936-x.
[11] C. Engström, Spectra of Gurtin-Pipkin type of integro-differential equations and applications to waves in graded viscoelastic structures, J. Math. Anal. Appl. 499 (2) (2021) 125063, 14, http://dx.doi.org/10.1016/j.jmaa.2021.125063, URL https://doi.org/10.1016/j.jmaa.2021.125063.
[12] J.A.C. Weideman, Gauss-Hermite quadrature for the Bromwich integral, SIAM J. Numer. Anal. 57 (5) (2019) 2200–2216, http://dx.doi.org/10.1137/18M1196273, URL https://doi.org/10.1137/18M1196273.
[13] N. Guglielmi, M.a. López-Fernández, G. Nino, Numerical inverse Laplace transform for convection-diffusion equations, Math. Comp. 89 (323) (2020) 1161–1191, http://dx.doi.org/10.1090/mcom/3497, URL https://doi.org/10.1090/mcom/3497.
[14] J. Abate, P.P. Valkó, Multi-precision Laplace transform inversion, Internat. J. Numer. Methods Engrg. 60 (5) (2004) 979–993, http://dx.doi.org/10.1002/nme.995, URL https://onlinelibrary.wiley.com/doi/abs/10.1002/nme.995.
[15] S. Giani, E.J.C. Hall, An *a posteriori* error estimator for *hp*-adaptive discontinuous Galerkin methods for elliptic eigenvalue problems, Math. Models Methods Appl. Sci. 22 (10) (2012) 1250030, http://dx.doi.org/10.1142/S0218202512500303, 35, URL https://doi.org/10.1142/S0218202512500303.
[16] S. Giani, L. Grubišić, H. Hakula, J.S. Ovall, An a posteriori estimator of eigenvalue/eigenvector error for penalty-type discontinuous Galerkin methods, Appl. Math. Comput. 319 (2018) 562–574, http://dx.doi.org/10.1016/j.amc.2017.07.007, URL https://doi.org/10.1016/j.amc.2017.07.007.
[17] S. Larsson, F. Saedpanah, The continuous Galerkin method for an integro-differential equation modeling dynamic fractional order viscoelasticity, IMA J. Numer. Anal. 30 (4) (2010) 964–986, http://dx.doi.org/10.1093/imanum/drp014, URL https://doi.org/10.1093/imanum/drp014.
[18] K. Mustapha, H. Brunner, H. Mustapha, D. Schötzau, An *hp*-version discontinuous Galerkin method for integro-differential equations of parabolic type, SIAM J. Numer. Anal. 49 (4) (2011) 1369–1396, http://dx.doi.org/10.1137/100797114, URL https://doi.org/10.1137/100797114.
[19] C. Effenberger, D. Kressner, C. Engström, Linearization techniques for band structure calculations in absorbing photonic crystals, Internat. J. Numer. Methods Engrg. 89 (2) (2012) 180–191, http://dx.doi.org/10.1002/nme.3235, URL https://doi.org/10.1002/nme.3235.